Available online at www.sciencedirect.com
SCIENCE DIRECT®
Thermochimica Acta 401 (2003) 63–75
thermochimica acta
www.elsevier.com/locate/tca

The construction and evaluation of a high pressure manifold and vessels for a Calvet type microcalorimeter☆

D.E.G. Jones*, A.-M. Turcotte, R.C. Fouchard

Canadian Explosives Research Laboratory, Natural Resources Canada, 555 Booth Street, Ottawa, Ont., Canada K1A 0G1

Received 26 July 2002; received in revised form 30 December 2002; accepted 31 December 2002

Abstract

A Setaram C-80 calorimeter has been modified in order to measure the heat flow of energetic materials at pressures up to 69 MPa. A manifold and sample cells capable of operating at high pressure were designed, constructed and evaluated. This paper will describe, in detail, the high pressure manifold construction, safety assessment and calibration. As well, the results for initial trials with ammonium nitrate (AN), and pentaerythritol tetranitrate (PETN) at various pressures and heating rates will be discussed.

Keywords: Evaluation; High pressure manifold; Calvet microcalorimeter; Ammonium nitrate; PETN

1. Introduction

Randzio [1] has recently reviewed developments in calorimetry and, in particular, has described the use of heat flow calorimetry (HFC) with pressure as a variable in investigations of phase transitions. He has outlined application of pressure studies to determination of characteristics of phase transitions and has provided several specific examples. In evaluation of the phase transitions of energetic materials (EM), techniques other than HFC have generally been used. For example, the phase behavior of ammonium nitrate (AN) has been determined using X-ray [2], Raman scattering [3] and DTA studies [4] at elevated pressures and that for ammonium dinitramide [5] using a high-temperature, high-pressure diamond anvil cell in conjunction with various spectroscopic techniques.

Reaction studies, using HFC, can be applied to simultaneously obtain kinetic and thermodynamic information [1] and, in combination with pressure studies can be used to evaluate the effect of high pressure on the decomposition behavior of EM, an important safety consideration for manufacture, transport, storage and use of these materials. Some early pressure studies have led to the evaluation of the kinetics of decomposition of EM. Brower [6] has investigated the effect of pressure on the decomposition of AN by means of a stainless steel reactor and evaluated the activation volume $\Delta V^{\ddagger}$ in the temperature range for an expected change in mechanism of AN decomposition. The effect of pressure on the thermal decomposition of several EMs has been studied using a diamond anvil high pressure cell [7] and it was shown that the rates of decomposition for β HMX and RDX decreased with increasing pressure while that for nitromethane increased.

☆ Presented at the Third International Heat Flow Calorimetry for Energetics Symposium, French Lick, IN, USA, 8–11 April 2002.

* Corresponding author. Tel.: +1-613-995-2140; fax: +1-613-995-1230.
E-mail address: djones@nrcan.gc.ca (D.E.G. Jones).

0040-6031/03/$ – see front matter © 2003 Published by Elsevier Science B.V.
doi:10.1016/S0040-6031(03)00056-X

This paper describes a system including high pressure manifold and cells for use with a Tian-Calvet microcalorimeter (Setaram C-80). This system has been specifically designed and constructed to allow for safe determination of the thermal properties of EM at various pressures up to 69 MPa. The performance of the C-80 in this environment has been determined and a preliminary study of the system behavior has been undertaken by experimental studies of the phase transitions of AN and the decomposition of pentaerythritol tetranitrate (PETN).

2. Experimental

2.1. Materials

Alumina (synthetic sapphire), indium and tin (SRM) were purchased from the National Bureau of Standards (NBS). Ammonium nitrate was ACS reagent grade (Sigma) and was dried overnight in an oven at 80 °C, then stored in a dessicator. Pentaerythritol tetranitrate, reported as better than 99 mass% purity, was removed from "liteline" detonating cord (Austin Powder Co.) and used directly.

2.2. Design and construction of the C-80 high pressure manifold

Extensive modifications to our Setaram C-80 heat-flux calorimeter were necessary to allow the study of the thermal decomposition of energetic materials at pressures up to 69 MPa. A picture of the complete system is shown in Fig. 1.

The Setaram C-80 consists of a massive aluminum block, with two identical cylindrical cavities located symmetrically about the center; a thermopile surrounds each cavity. The design results in a sensitivity to heat flow of about 10 μW. This sensitivity, the ability to heat at very low heating rates $\beta = 0.01$–$2.00\,^{\circ}\mathrm{C\,min^{-1}}$ and the ruggedness of the C-80 make it an ideal candidate for high pressure applications.

All components of the high pressure manifold were rated at > 69 MPa. Presently, a 41.3 MPa argon cylinder is being used as a pressure source and a maximum pressure of 33 MPa is being used. Following a complete evaluation of the system, a pressure source capable of reaching 69 MPa will be incorporated.

A 13 mm thick "Lexan" cage was constructed around the apparatus, with an exhaust vent. This cage protects the operator from mishaps and/or fumes. Pressure sample/reference vessels are available from Setaram, however, these vessels have a wall thickness of 3.1 mm and are limited to a maximum pressure of 10 MPa. Therefore, high pressure sample/reference vessels and transfer tubes were manufactured by our machine shop. These vessels were made from 316 stainless steel with a wall thickness of 5.25 mm, and a volume of 3.26 mL. The transfer tubes were constructed using 6 mm 316 stainless steel tubing with a wall thickness of 2 mm capable of withstanding a maximum pressure of 80 MPa. The vessels and transfer tubes were connected with 6 mm "swagelok" fittings using silver-coated front ferrules. This system gave an excellent seal over 8–10 experiments, at which point, a new fitting and ferrule could be installed without replacing the entire transfer tube. Fig. 2 shows details of the vessels and transfer tubes designed and constructed at our facility. The transfer tubes were connected to the high pressure manifold using 3 mm o.d. × 1 mm i.d. tubing. This allowed a "flexible" connection between the sample/reference vessels and manifold without compromising the pressure limits. A schematic for the high pressure manifold is shown in Fig. 3.

The total volume of the system (vessels, transfer tubes plus the manifold) was calculated to be 28.3 mL. All components of the manifold have maximum pressure ratings greater than 69 MPa. As an added safety precaution, air actuated valves (Autoclave Engineers) were installed for the gas inlet, outlet and sample vessel. These valves are controlled using solenoid valves (Snap-Tite) connected to a control box with a long cable to allow remote manipulation. Flushing and pressurization of the manifold/vessels, can therefore be carried out at a safe distance from the apparatus. A pressure relief valve (Autoclave Engineers) set at 70 MPa was installed as a further safety precaution.

A series of pressure transducers with 4–20 mA output (Setra Systems Inc.) were purchased to cover the pressure range from 0 to 69 MPa. These transducers can easily be interchanged to cover the pressure range of interest. The pressure transducer was connected to a digital panel meter (Alpha Control & Instruments). In order to store the pressure data, the digital meter was connected to a "Strawberry Tree" data shuttle

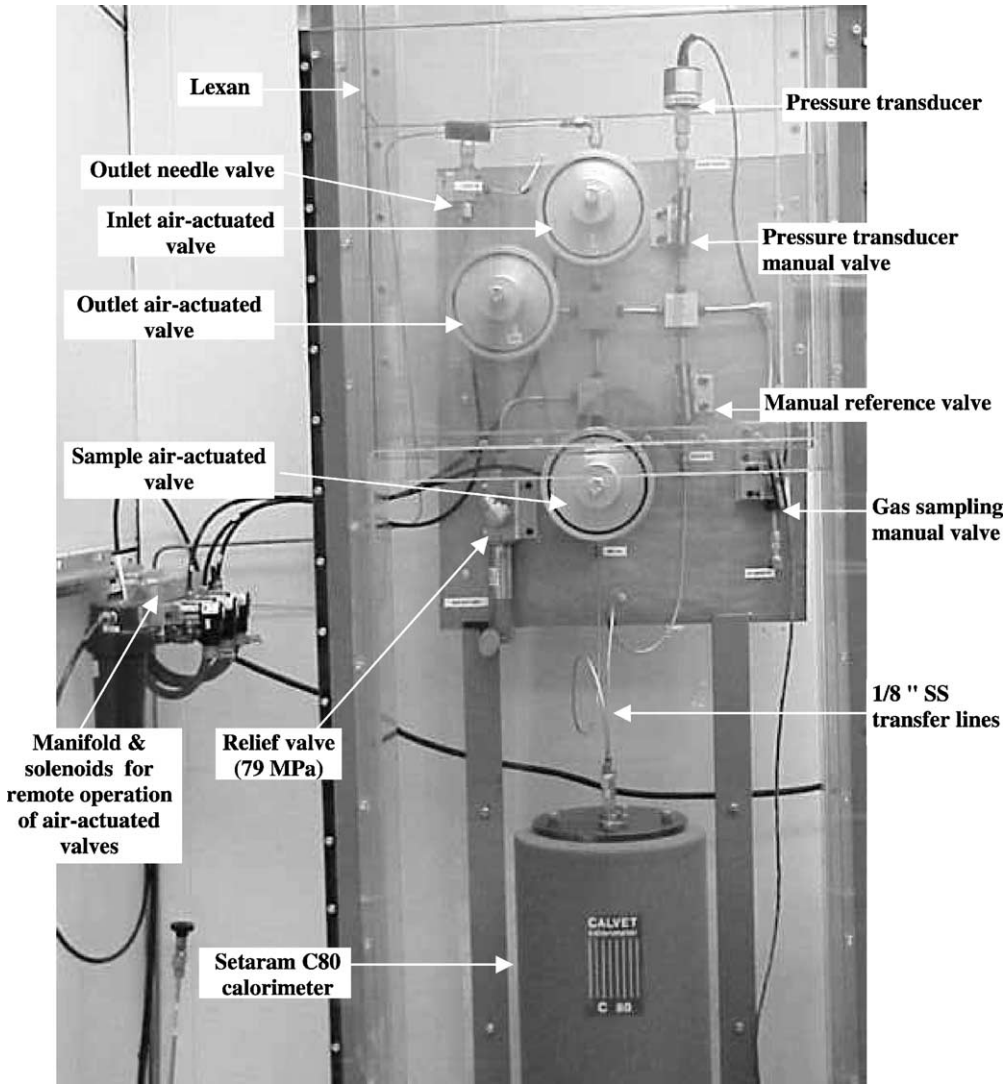

Fig. 1. Photography of the pressure manifold attached to the C-80 heat-flux calorimeter.

(Dalimar Instruments Inc.) then to a computer utilizing the "Workbench PC for Windows" software (Adept Scientific). At the end of an experiment the C-80 heat flow data and pressure data files were combined using "Sigma-Plot" software (SPSS Inc.).

To protect the sample vessel from corrosion, alumina liners (99.7 %) (Arklay S. Richards Co. Inc.) were used. The liners were 6 mm o.d. × 4 mm i.d. and 90 mm high. For very fine samples 6 mm o.d. extra coarse (170–220 μm) fritted discs were placed on top of the sample liner to contain the sample during the experiment.

A detailed operating procedure, and a safety assessment were developed for the complete system before any experimental work was started. Calculation of the effects of overpressure in the system as well as an evaluation of fragmentation hazards were carried out as part of the safety assessment. The overpressure likely to be generated if a sample of explosive were to burn to completion in the C-80 while operating at high

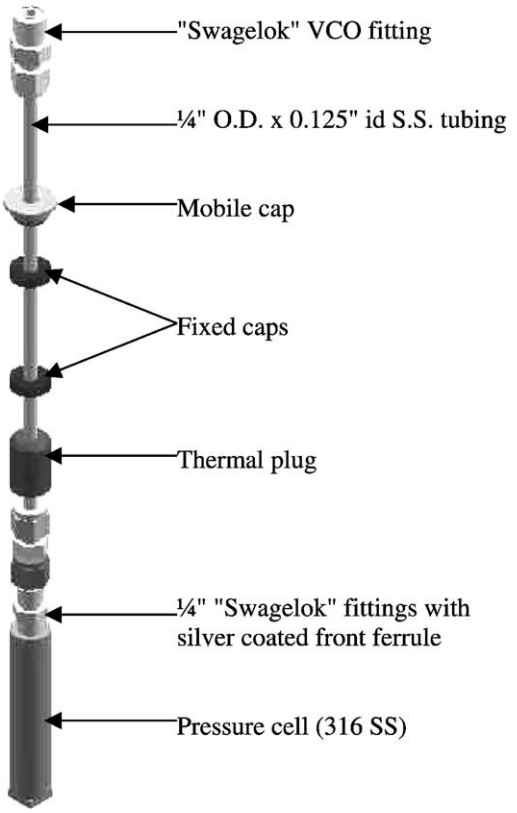

Fig. 2. Schematic of the high pressure cells and connections to the manifold.

pressure was estimated. The example used for this calculation was the rapid burning of 0.1 g of the explosive HMX, where all of the heat generated goes to pressurizing the 69 MPa of argon initially in the system (an extreme case). At the present time, we are limiting the system to a maximum sample mass of 0.1 g of energetic material to a maximum temperature of 300 °C (the upper temperature limit of the C-80). Under these conditions, at a starting pressure of 69 MPa the calculations show that the overpressure from the reaction would be 80 MPa. This is slightly above the 79.2 MPa setting for the relief valve and within the limits of the system.

Calculations were also carried out to ascertain the fragmentation hazard of a failure of a part of the system. The weakest point of the system was assumed to be the 0.125 in. (0.3 cm) tubing between the vessel and the manifold. Assuming that the largest fragment would be a 10 cm half segment of this tubing, having a mass of 2.4 g, and assuming that this fragment would reach a velocity of the speed of sound in argon (322 m s^{-1}), then the kinetic energy would be 124 J. The specifications of the Lexan cage state that it is capable of withstanding these levels of forces.

The connection between the sample vessel and the transfer tube is the most critical since it must be opened and re-tightened for every run. It was difficult to maintain a leak-free connection for more than one or two experiments with stainless steel front ferrules. Switching to silver-coated front ferrules gave a much better and more durable seal. At that point, a whole new fitting was installed. The "VCO" fittings between the transfer tubes and 0.3 cm tubing to the manifold also have to be opened and re-tightened for every run. However, this connection, which is not heated, could be reused over many runs with only occasional replacement of the "O" ring.

The system was leak tested, and calibration of the temperature and heat flow was carried out. Baseline experiments at various pressures, a repeatability study and verification using indium were completed. Preliminary studies with AN and PETN were then conducted.

2.3. Leak testing

The system was first pressurized to 3.4 MPa with argon and monitored for leaks. Once the system was leak tight the system was pressurized to 34.5 MPa and monitored. This procedure was repeated until the system was free of leaks. During the initial testing, leaks developed at the fitting between the cell and transfer tubes. With the silver-coated ferrules, a leak-free connection could be maintained for eight or nine experiments before needing replacement.

2.4. Calibration

The first step of calibration was verification of the thermocouples. A 45 cm type K thermocouple (Omega) was calibrated against a temperature calibrator (Fluke 701). This thermocouple was placed in the sample well of the C-80. The instrument was heated to 25 °C and held there for 2 h. Readings of the block, furnace and sample thermocouple were recorded at the end of the 2 h wait time. This procedure was repeated at 100, 200, and 300 °C. The differences between the block temperature

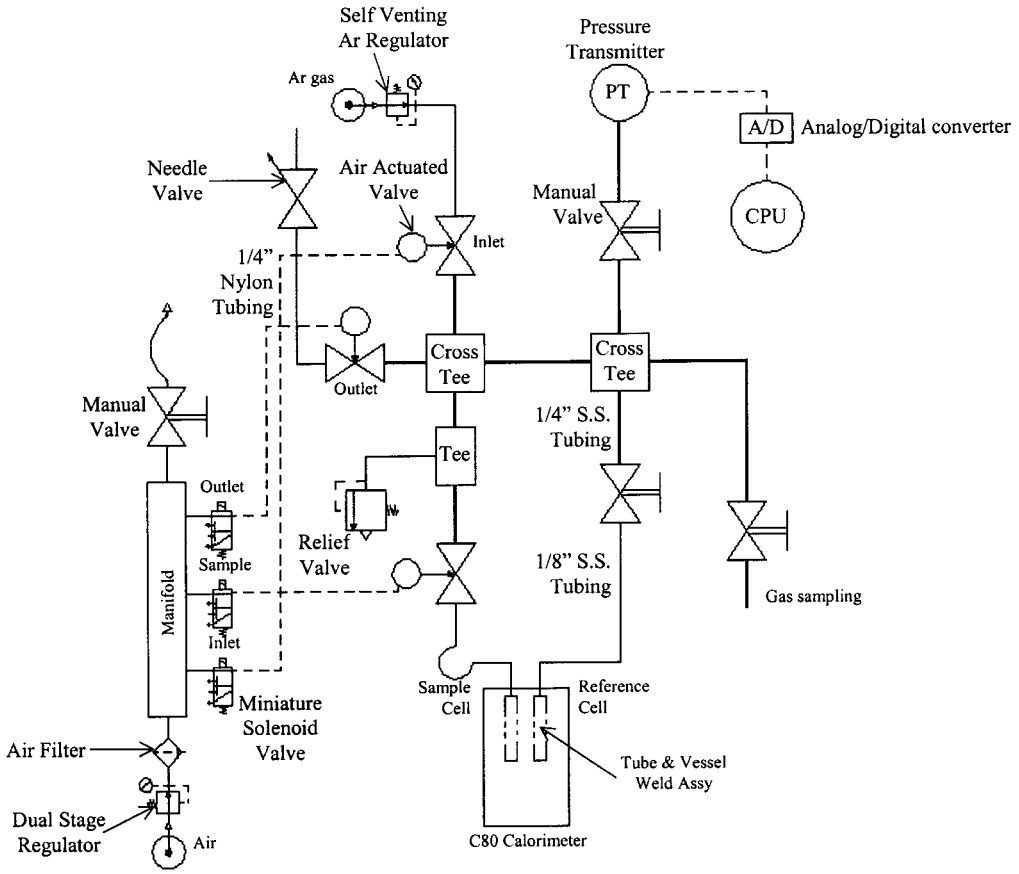

Fig. 3. Schematic for the high pressure manifold.

and the corrected sample temperature values were used as temperature correction factors in the C-80 software.

The results for the verification and calibration of the C-80 thermocouples are shown in Table 1. The sample temperature (T) correction is the difference between the block temperature and the sample temperature measured by placing a calibrated thermocouple in the sample vessel well. These values were used to adjust the C-80 temperature calibration for the new high pressure sample/reference vessels.

Baseline experiments with empty vessels at 0.3 °C min^{-1} and 0.17 and 33.2 MPa argon were then carried out, as well as a run with sapphire (4 g) at the same heating rate and ambient pressure. The graph for the baseline experiment at 33.2 MPa argon is shown

Table 1
Verification and calibration of the C-80 thermocouples at the block, furnace and sample

Program T/°C	Block T/°C	Furnace T/°C	Sample T/°C	Sample T/°C correction
25	24.97	25.45	24.9	−0.07
100	98.86	99.99	99.6	+0.74
200	197.97	200.00	198.6	+0.63
300	297.12	300.00	297.9	+0.78

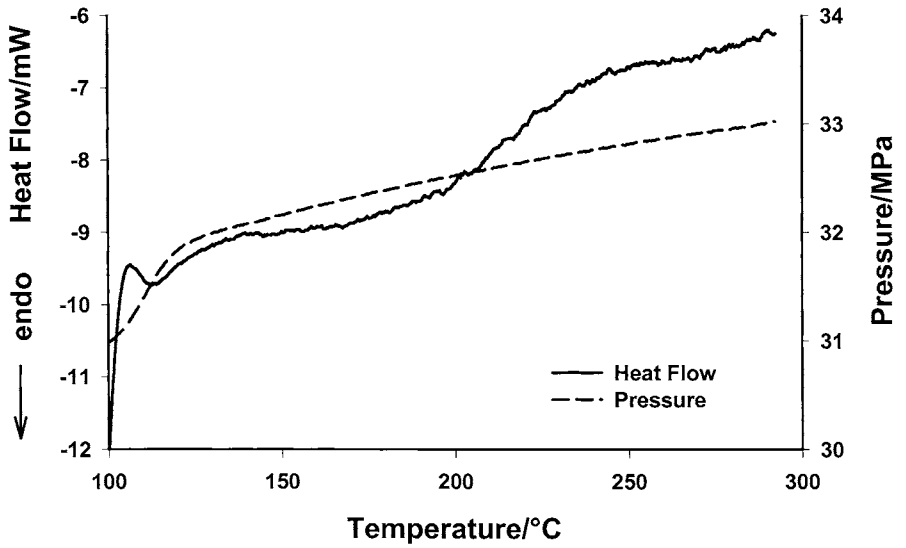

Fig. 4. Baseline experiment at ~33 MPa argon.

in Fig. 4. The baseline drift over the temperature range 100–300 °C was less than 4.0 mW.

The thermal mass of the new pressure cells is quite high (140 g versus 75 g for standard cells), therefore the system is probably not at equilibrium using a heating rate of 0.3 °C min^{-1}. Results of a repeatability study using indium at 0.3 °C min^{-1} and 0.17 MPa argon to verify the calibration of the high pressure system are shown in Table 2. Three samples of indium were run and the results compared. The onset temperature values are too high and the enthalpy values are low.

It was decided that the original Setaram factory calibration would be used and corrected using experiments with indium and tin reference materials (SRM) at five different heating rates and various pressures up to about 30 MPa. These experiments were performed as follows: 100 mg of indium was placed in an alumina liner, about 75 mg of alumina powder was placed on top of the indium and 100 mg of tin was placed on top of the alumina. In this way, both SRM materials could be analyzed in one experiment. These materials were run at $\beta = 0.1$, 0.3, 0.5, 0.7, and 1.0 °C min^{-1} and various pressures up to about 32 MPa. The values of the onset temperature T_o and the enthalpy of fusion, ΔH_{fus} for both indium and tin at the five heating rates and $p = 0.17$ MPa are given in Table 3.

The average heat of fusion, based on the five heating rates for each metal was used to calculate a factor F using the equation: $F =$ (true ΔH_{fus})/(experimental

Table 2
Results for the repeatability of the onset temperature T_o and the enthalpy of fusion ΔH_{fus} of indium reference material at $\beta = 0.3$ °C min^{-1}

T_o/°C	ΔH_{fus}/J g^{-1}
159.05	26.2
158.88	26.4
159.21	26.3

Literature values, 156.6 °C and 28.7 J g^{-1}.

Table 3
Results for the onset temperature T_o and the enthalpy of fusion ΔH_{fus} of indium and tin at different heating rates β

β/°C min^{-1}	T_o/°C	ΔH_{fus}/J g^{-1}
Indium		
1.0	163.2	25.0
0.7	161.4	26.0
0.5	159.9	27.7
0.3	158.7	26.1
0.1	157.2	26.1
Tin		
1.0	238.6	53.0
0.7	236.6	53.9
0.5	235.2	55.4
0.3	233.9	57.3
0.1	232.3	55.6

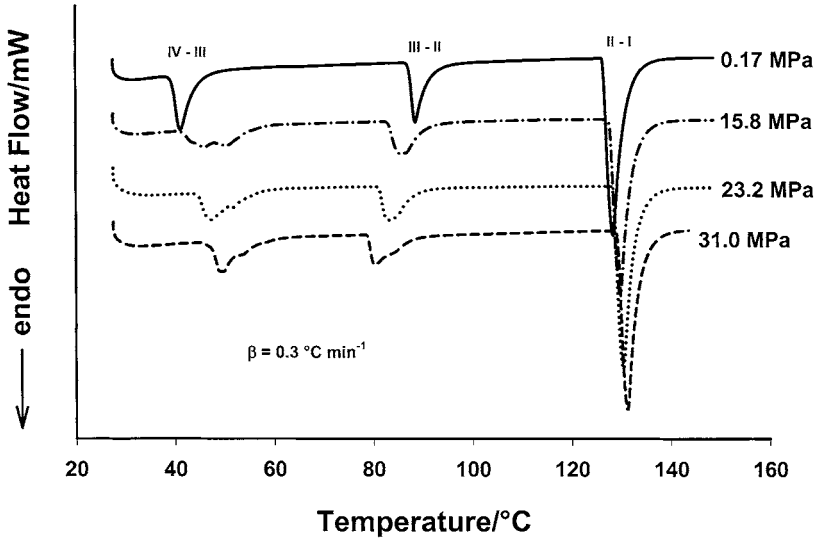

Fig. 5. Comparison of the heat flows for ammonium nitrate (AN) at various pressures of argon.

Table 4
Onset temperatures T_o and enthalpy changes ΔH for phase transitions of AN

Phase transition	T_o/°C		ΔH/J g^{-1}	
	This work	Literature	This work	Literature
IV–III	42.1	43–51 [9]	16.63 ± 0.40	16–20 [9]
III–II	86.7	86.0 [9]	16.3[a]	15.5–16.8 [9]
II–I	126.4	125.2 [10]	55.53 ± 0.37	54.99 ± 0.30 [10]

[a] Pressure dependant.

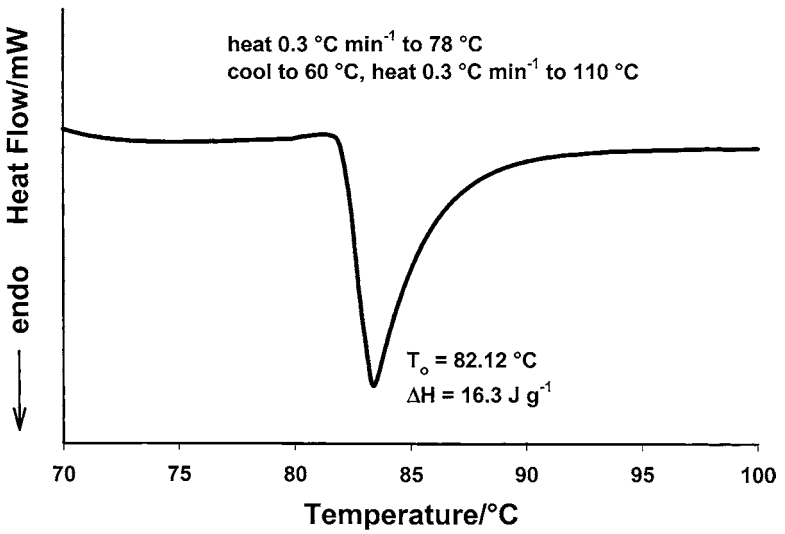

Fig. 6. Heat flow for “conditioned” AN at 31.1 MPa argon.

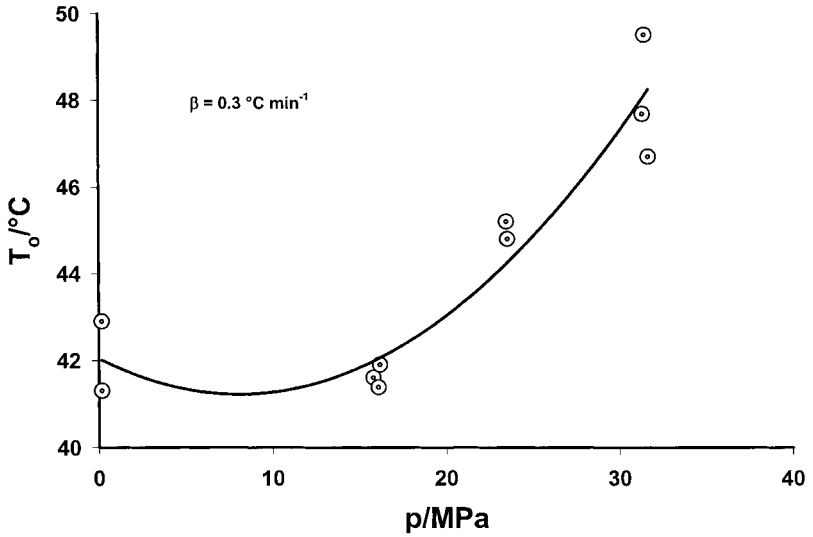

Fig. 7. Pressure dependence of the onset temperature T_o for AN IV–III phase transition.

ΔH_{fus}). The factors for the two metals were averaged and each sensitivity coefficient was divided by the factor F, to determine new coefficients.

In the same way, the onset temperatures were used to correct the temperature coefficients in the C-80 software. An experiment using indium and tin at 0.3 °C min^{-1} and 0.17 MPa argon was carried out to verify the temperature and heat flow calibration values. The T_o and ΔH_{fus} values for indium (156.7 °C and 29.0 J g^{-1}) were in good agreement with the literature values of 156.6 °C and 28.7 J g^{-1}. Likewise, the values for tin (231.8 °C and 60.1 J g^{-1}) agreed well with the literature values of 231.97 °C and 60.2 J g^{-1}. The large thermal mass of the high pressure cells was

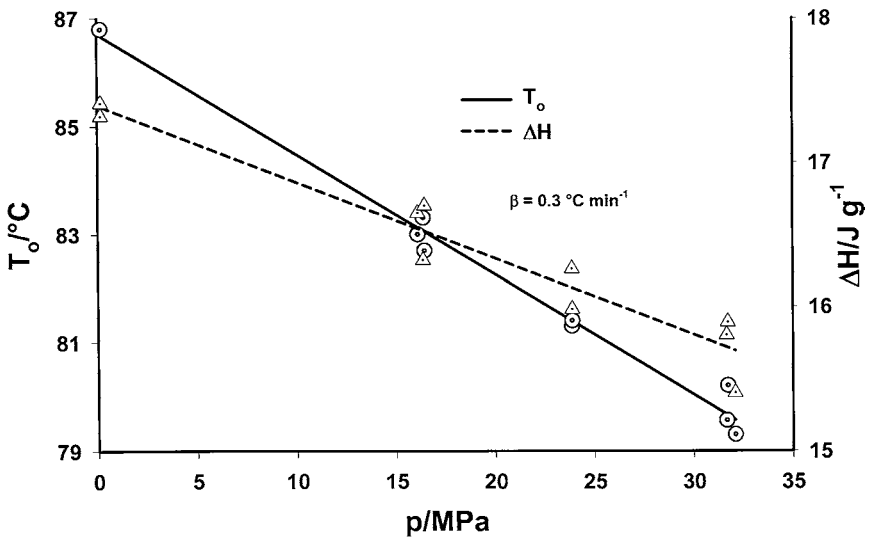

Fig. 8. Pressure dependence of the onset temperature T_o and ΔH for AN III–II phase transition.

compensated for with the calibration technique described above and the system was now ready for trials with energetic materials. The pressure coefficients for T_o and ΔH_{fus} of indium and tin were negligibly small and were not used to correct for pressure effects on the calibration.

3. Results and discussion

3.1. AN trials

As an initial test of the pressure manifold, a study was undertaken to examine the effect of pressure on the phase transitions of AN. Samples of 0.8 g dry AN were heated from 28 to 150 °C at 0.3 °C min^{-1} at $p =$ 0.17, 15.8, 23.0, and 31.0 MPa of argon. An overlay graph of representative experiments is shown in Fig. 5. Table 4 compares T_o and ΔH for the phase transitions IV–III, III–II and II–I, with those reported in the literature. Wide variation in the literature data, particularly for the IV–III and III–II transitions, is a result of different thermal history and moisture content of the AN samples.

The AN IV–III and III–II phase transition peaks at higher pressures were very irregular in shape, unlike those at ambient pressure. These transitions are known to be very slow because of the drastic crystallographic changes occurring [8]. Hence, it was felt that an annealing period would allow structural relaxation and a sharper transition might occur. In order to test this idea, a run of 0.8 g AN at 31.1 MPa of argon was carried

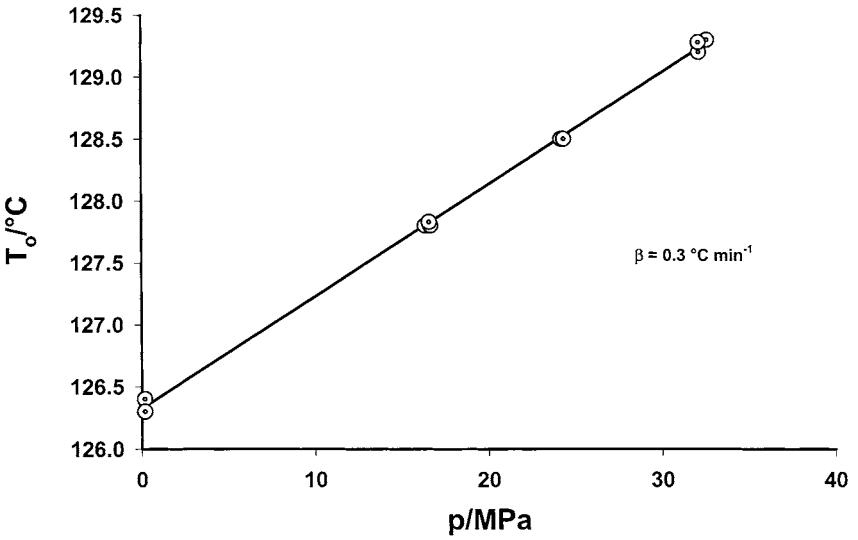

Fig. 9. Pressure dependence of the onset temperature T_o for AN II–I phase transition.

Table 5
Regression coefficients A and B for fit of Eq. (1) and comparison of values of ΔV from this work and those from literature

Phase transition	A	$10^2\ B$/MPa	R^2	$10^2\ \Delta V$/cm^3 mol^{-1}	
				This work	[4]
IV–III (p > 15 MPa)	35.2 ± 1.1	41.1 ± 4.6	0.93	173 ± 18	164 ± 7
III–II	86.72 ± 0.17	−22.30 ± 0.77	0.99	−82.4 ± 3.3	−78 ± 9
	17.39 ± 0.11	−5.31 ± 0.50	0.93		
II–I	126.32 ± 0.02	9.06 ± 0.11	1.00	100.7 ± 1.2	88 ± 2

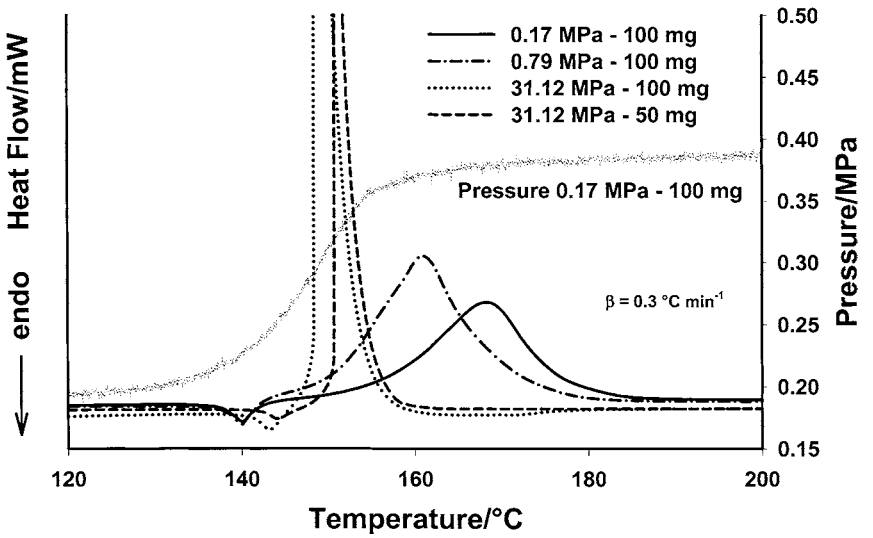

Fig. 10. Comparison of the heat flows for PETN at various pressures of argon.

out with "conditioning" steps before the measurement of the AN III to II phase transition as follows:

- heat at 0.3 °C min^{-1} to 78 °C;
- cool to 60 °C, heat at 0.3 °C min^{-1} to 110 °C.

The results of this experiment are shown in Fig. 6. As can be seen from this figure, the "conditioning" produced a smooth and regular peak.

The initial trials to examine the effect of pressure on the phase transitions of AN showed substantial shifts in the onset temperatures T_o of the transitions with pressure (Fig. 5). Plots of T_o (and ΔH for the III–II transition) versus pressure p are shown in Figs. 7–9, and Table 5 provides a summary of the results obtained for fitting the equation:

$$X = A + Bp \quad (1)$$

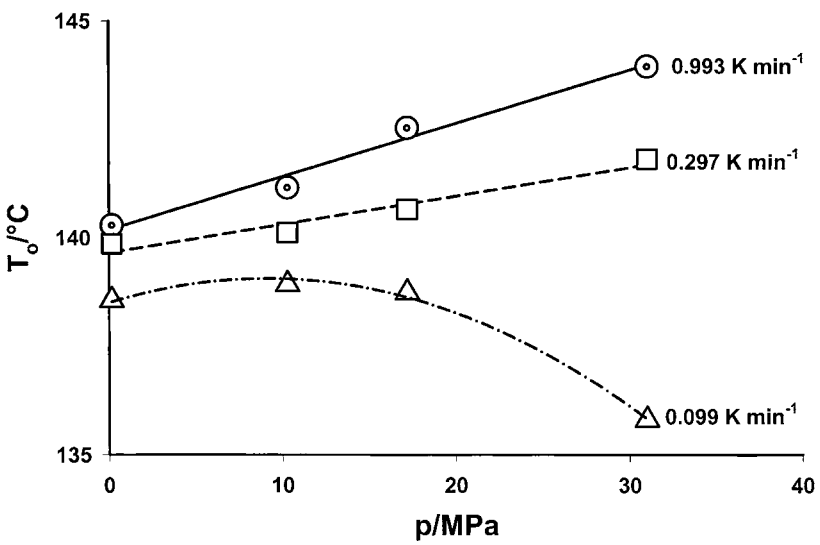

Fig. 11. Pressure and heating rate dependence of the onset temperature T_o of fusion for PETN.

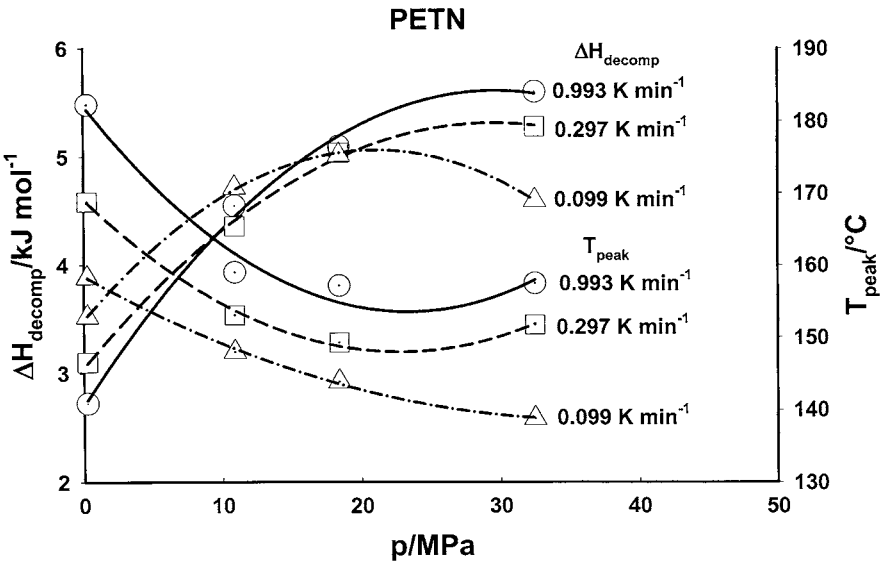

Fig. 12. Pressure and heating rate dependence of the enthalpy ΔH_{decomp} and peak temperature T_{peak} for decomposition of PETN.

where $X = T_o/°C$ and $\Delta H/J\,g^{-1}$ (III–II transition). As well, the volume changes ΔV estimated from the pressure dependence of T_o, using the Clausius–Clapeyron equation, are included in Table 5 and compared with those values of ΔV determined from dT_o/dp data calculated from phase diagram information for AN [4], obtained using a DTA apparatus at pressures up to 600 MPa. The agreement between our results and those obtained from the data of Jain and Chaubey [4] is generally good.

From the regression coefficient B in Table 5 for the dependence of ΔH on pressure for the III–II transition, the pressure coefficient $d(\Delta H)/dp$ is $-4.12 \pm 0.41\,cm^3\,mol^{-1}$.

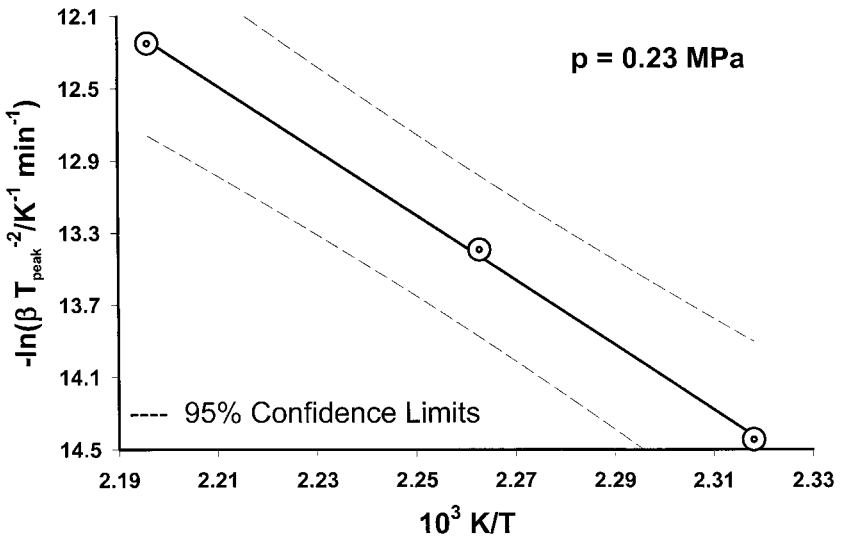

Fig. 13. Plot of $-\ln(\beta\, T_{\text{peak}}^{-2}/K^{-1}\,min^{-1})$ vs. $10^3\,K/T$ for PETN at 0.23 MPa.

3.2. PETN trials

To evaluate the performance of the high pressure manifold at higher temperatures, during decomposition of energetic materials, a study was undertaken using PETN. Initially, samples of 100 mg of PETN were heated from 28 to 300 °C at $\beta = 0.3\,^{\circ}\mathrm{C\,min^{-1}}$. At higher pressures the C-80 detector signal was saturated, therefore the sample size was reduced to 50 mg. A comparison of the results at $p = 0.17$, 0.79 and 31 MPa of argon is shown in Fig. 10. The onset temperature T_o of fusion for PETN at 0.17 MPa was $139 \pm 1\,^{\circ}\mathrm{C}$ and $\Delta H_{fus} = 176 \pm 10\,\mathrm{J\,g^{-1}}$ compared with literature values [11] of 141 °C and $156\,\mathrm{J\,g^{-1}}$, respectively. It should be noted that the enthalpy of decomposition, ΔH_{decomp}, which is $2.9 \pm 0.2\,\mathrm{kJ\,g^{-1}}$ at $p = 0.17$ MPa, increases significantly with pressure, approaching that of the enthalpy of explosion, $5.9\,\mathrm{kJ\,g^{-1}}$ [11]. DSC studies for samples of PETN confined in a sealed glass ampoule with an internal volume of about $5\,\mathrm{mm^3}$ gave $\Delta H_{decomp} = 4.1\,\mathrm{kJ\,g^{-1}}$ [12].

The thermal behavior of PETN was determined up to 300 °C to test the high pressure manifold during decomposition. At various pressures of argon, substantial differences in T_o, ΔH_{fus} and ΔH_{decomp} were observed (Fig. 10). Plots for the melting endotherm and decomposition exotherm of PETN at the various heating rates β and pressures p are shown in Figs. 10 and 11.

The onset temperature T_o of fusion for PETN show a linear increase with increasing pressure at $\beta = 0.993$ and $0.297\,^{\circ}\mathrm{C\,min^{-1}}$, however, at a heating rate of $0.099\,^{\circ}\mathrm{C\,min^{-1}}$, T_o appears to decrease with increasing pressure (Fig. 11). The ΔH_{decomp} values and peak temperatures T_{peak} for the decomposition of PETN versus pressure at the three heating rates are shown in Fig. 12. At ambient pressure, ΔH_{decomp} decreases and T_{peak} increases with increase in the heating rate β. T_{peak} decreases and ΔH_{decomp} increases with increasing pressure.

An example plot of $-\ln(\beta\, T_{peak}^{-2})$ ($\mathrm{K^{-1}\,min^{-1}}$) versus $10^3 T$ (K) at $p = 0.23$ MPa is shown in Fig. 13. Values of $E = 149\,\mathrm{kJ\,mol^{-1}}$ and $\ln(Z/\mathrm{s^{-1}}) = 23.1$ were determined, compared with the literature values [13] of $E = 197\,\mathrm{kJ\,mol^{-1}}$ and $\ln(Z/\mathrm{s^{-1}}) = 37.1$. In this manner, apparent first order rate constants at 420 K were estimated from the heating rate studies at the various pressures and these results are recorded in Table 6. While there is considerable uncertainty in the results, especially at high pressures, it appears that $\Delta \ln k/\Delta p > 0$ and therefore $\Delta V^{\ddagger} < 0$, where $\Delta V^{\ddagger}$ is the volume of activation for the decomposition of PETN. Such a decrease in volume on going to the activated state is suggestive of an ionic mechanism for the decomposition in contrast with the previously proposed homolytic mechanism [14] at ambient pressure.

Table 6
Arrhenius parameters and rate constant k as function of pressure for PETN

p/MPa	$\ln(Z/\mathrm{s^{-1}})$	E/kJ mol^{-1}	$-\ln(k/\mathrm{s^{-1}})$[a]
0.23	23.1	149	19.7 ± 4.3
11.20	69.7	309	18.7 ± 5.1
18.50	53.6	250	18 ± 31
31.00	29.5	165	18 ± 72

[a] At 420 K.

4. Conclusions

The high pressure manifold designed and constructed at our facility has enhanced our ability to thermally characterize energetic materials. By carefully choosing components that exceeded the pressure limits required, carrying out a detailed safety assessment of the system and testing and verifying the system in stages, it was shown that the manifold can be operated safely and effectively. The large mass of the sample/reference vessels necessary at high pressures means that calibration of the system to account for thermal lag and use of lower heating rates are necessary to take full advantage of this system.

This instrumentation allows examination of the pressure effect on phase transitions, allowing the determination of ΔV values as demonstrated with the experiments carried out in this study using AN. The onset temperature of melting of PETN increases with pressure, except at very low heating rates. The enthalpy values for the decomposition of PETN increase with increasing pressure and the peak temperature decreases with increasing pressure.

Acknowledgements

Ettore Contestabile and Don Wilson of the Canadian Explosives Research Laboratory (Natural Resources

Canada) provided valuable information for the vessel design and commissioning of the manifold. The authors would also like to thank Al Vaillancourt and Sal Alaimo from Technical Services at Natural Resources Canada, for their valuable assistance in assembling the manifold.

References

[1] S.L. Randzio, Annu. Rep. Prog. Chem. Sect. C 998 (1998) 433.
[2] Y. Shinnaka, I. Sasaki, S. Yamamoto, T. Kaneda, J. Phys. Soc. Jpn 58 (1989) 1644.
[3] J. Medina, W.F. Sherman, G.R. Wilkinson, in: Proceedings of the Eighth International Conference on Raman Spectroscopy, Bourdeaux, France, 1982, p. 401.
[4] P.C. Jain, D. Chaubey, in: Proceedings of the International Conference on Thermal Analysis, Therm. Anal., Bayreuth, Germany 6 (1980) 335.
[5] T.P. Russell, G.J. Piermarini, S. Block, P.J. Miller, J. Phys. Chem. 100 (1996) 3248.
[6] K.R. Brower, in: Proceedings of the Eighth Symposium on Chemical Problems Connected with Stabilized Explosives, Strömstad, Sweden, 1988, p. 273.
[7] G.J. Piermarini, S. Block, P.J. Miller, in: Proceedings of the 19th International Conference of ICT on Combustion and Detonation Phenomena, Karlsrühe, Germany, 29 June–1 July 1988.
[8] D.C. Sorescu, D.L. Thompson, J. Phys. Chem. 105 (2001) 720.
[9] E. Kestila, J. Valkonen, Thermochim. Acta 214 (1993) 305.
[10] H. Langfelderova, P. Ambrovic, Thermochim. Acta 56 (1982) 385.
[11] J. Kohler, R. Meyers, Explosives, 4th revised and extended ed., VCH, Chichester, 1993.
[12] D.E.G. Jones, R.A. Augsten, Thermochim. Acta 286 (1996) 355.
[13] A.J. Robertson, J. Soc. Chem. Ind. 67 (1948) 221.
[14] M.J. Hiskey, K.R. Brower, J.C. Oxley, J. Phys. Chem. 95 (1991) 3955.